

## Giant magnetoelectric effect in the $J_{\text{eff}}=1/2$ Mott insulator $\text{Sr}_2\text{IrO}_4$

S. Chikara,<sup>1,2</sup> O. Korneta,<sup>1,2</sup> W. P. Crummett,<sup>1,3</sup> L. E. DeLong,<sup>1,2</sup> P. Schlottmann,<sup>4</sup> and G. Cao<sup>1,2,\*</sup>

<sup>1</sup>Center for Advanced Materials, University of Kentucky, Lexington, Kentucky 40506, USA

<sup>2</sup>Department of Physics and Astronomy, University of Kentucky, Lexington, Kentucky 40506, USA

<sup>3</sup>Science Division, Centre College, Danville, Kentucky 40422, USA

<sup>4</sup>Department of Physics, Florida State University, Tallahassee, Florida 32306, USA

(Received 5 August 2009; published 19 October 2009)

Our magnetic, electrical, and thermal measurements on single crystals of the  $J_{\text{eff}}=1/2$  Mott insulator,  $\text{Sr}_2\text{IrO}_4$ , reveal a giant magnetoelectric effect (GME) arising from a frustrated magnetic/ferroelectric state whose signatures are: (1) a strongly enhanced electric permittivity that peaks near an observed magnetic anomaly at 100 K, and (2) a large ( $\sim 100\%$ ) magnetodielectric shift that occurs near a metamagnetic transition. The GME hinges on a spin-orbit gapping of  $5d$  bands rather than the magnitude and spatial dependence of magnetization, as traditionally accepted.

DOI: 10.1103/PhysRevB.80.140407

PACS number(s): 75.80.+q, 75.30.Kz, 75.70.-i, 78.20.Ci

It is commonly expected that iridates are more metallic and less magnetic than their  $3d$ ,  $4d$ , and  $4f$  counterparts. The extended nature of the  $5d$  orbitals leads to a broader  $5d$ -bandwidth  $W$  and a reduced Coulomb interaction  $U$  such that  $Ug(E_F) < 1$ , where  $g(E_F)$  is the density of states; the Stoner criterion therefore anticipates a metallic, paramagnetic state. In marked contrast, many iridates are magnetic insulators with exotic properties,<sup>1–12</sup> such as the coexistence of a charge density wave and weak ferromagnetism (FM) in  $\text{BaIrO}_3$ ,<sup>1–3</sup> anomalous “diamagnetism” in  $\text{Sr}_3\text{Ir}_2\text{O}_7$ ,<sup>10</sup> and  $J_{\text{eff}}=1/2$  Mott state in  $\text{Sr}_2\text{IrO}_4$ .<sup>9,11</sup> Strong spin-orbit coupling ( $\sim 0.3$ – $0.4$  eV, compared to  $\sim 20$  meV in  $3d$  materials) competes with other interactions in  $5d$  materials to drive these exotic states.

In this Rapid Communication, we report dielectric, magnetic, transport and thermal properties of single-crystal  $\text{Sr}_2\text{IrO}_4$ . We observe a giant magnetoelectric effect (GME) characterized by a strongly peaked permittivity near an observed magnetic anomaly at 100 K, and a large magnetodielectric shift near a metamagnetic transition. The GME hinges on strong spin-orbit coupling rather than the magnitude and spatial dependence of magnetization, contrary to current phenomenological models.

In  $\text{Sr}_2\text{IrO}_4$ , strong crystal fields split off  $5d$  band states with  $e_g$  symmetry (which play only a secondary role in physical properties), and  $t_{2g}$  bands arise from  $J=1/2$  and  $J=3/2$  multiplets via strong spin-orbit coupling. A weak admixture of the  $e_g$  orbitals downshifts the  $J=3/2$  quadruplet from the  $J=1/2$  doublet.<sup>9</sup> An independent electron picture anticipates a metallic compound since the  $\text{Ir}^{4+}$  ( $5d^5$ ) ions provide four electrons to fill the lower  $J_{\text{eff}}=3/2$  bands, plus one electron to partially fill the  $J_{\text{eff}}=1/2$  bands.

Crucial to the present study of  $\text{Sr}_2\text{IrO}_4$  is that even a modest  $U$  ( $\sim 0.5$  eV) can induce a Mott insulating gap  $\Delta \sim 0.5$  eV (Refs. 9 and 11) in the  $J_{\text{eff}}=1/2$  band due to its narrow width ( $W=0.48$  eV), a circumstance that favors a recently predicted mechanism for a GME.<sup>12</sup> The GME is an established feature of  $3d$  multiferroics but previously unobserved in  $5d$  perovskites. Moreover, the traditional view is that GME depends only on the magnitude and spatial dependence of magnetization, whereas the mechanism suggests a

critical role of an effective spin-orbit gap  $\Delta_s$ .<sup>12</sup> Our results indicate this mechanism is realized in  $\text{Sr}_2\text{IrO}_4$ .

Synthesis and characterization of single-crystal  $\text{Sr}_2\text{IrO}_4$  are described elsewhere.<sup>7,10</sup> Measurements of specific heat  $C(T, H)$ , magnetization  $M(T, H)$ , ac susceptibility  $\chi(T, H, \omega)$ , and electrical resistivity  $\rho(T, H)$  for  $T < 400$  K were performed using either a Quantum Design physical properties measurement system or magnetic property measurement system. High-temperature thermoelectric power  $S$  and  $\rho$  were measured from 9 to 600 K. The complex permittivity  $\varepsilon(T, H, \omega) = \varepsilon' + i\varepsilon''$  was measured using a 7600 QuadTech LCR Meter with  $10 \text{ Hz} \leq \omega \leq 2 \text{ MHz}$  and  $H < 12$  T. The electric polarization was measured using a Radian Precision Premier II polarimeter.

The complex behavior of  $\text{Sr}_2\text{IrO}_4$  demands a careful comparison of single-crystal data for  $M(T)$ ,  $C(T)$ ,  $\rho(T)$ , and  $S(T)$ , as shown in Fig. 1. Our results agree with previous magnetic data for  $\text{Sr}_2\text{IrO}_4$ , which revealed weak FM order below  $T_C = 240$  K (Refs. 4–8) and a low-field metamagnetic transition resulting in a small saturation moment  $\mu_s < 0.13 \mu_B/\text{Ir}$  (sample dependent) along the easy  $\mathbf{a}$  axis.<sup>7</sup> The Curie-Weiss temperature  $\theta_{\text{CW}} = +236$  K extrapolated from the inverse susceptibility  $\Delta\chi^{-1}$  ( $\Delta\chi = \chi(T) - \chi_0$ , where  $\chi_0$  is a  $T$ -independent contribution) confirms FM exchange coupling over the range  $270 < T < 350$  K [Fig. 1(a)]. Arrott plots also corroborate weak FM order at  $T_C \approx 240$  K [Fig. 1(d) inset].

On the other hand,  $C(T < 11 \text{ K})$  is predominantly proportional to  $T^3$  at  $\mu_0 H = 0$  and 9 T [Fig. 1(b) inset] due to a Debye-phonon and/or magnon contributions from an anti-FM (AFM) ground state, in apparent conflict with the weak FM behavior suggested by Fig. 1(a). Indeed, the field shift [ $C(T, H) - C(T, 0)$ ]/ $C(T, 0) \sim 16\%$  at 9 T indicates a significant magnetic contribution to  $C(T)$  and suggests that a competition between AFM and FM exchange produces a low temperature  $C(T)$  consistent with AFM magnons. The relative strength of AFM and FM interactions clearly shifts to drive different magnetic states at high and low  $T$ , to which we return below. A tiny specific-heat anomaly ( $|\Delta C| \sim 4$  mJK/mole K) is observed at  $T_C$ , indicating a very small entropy change [Fig. 1(b)] [complete absence of a  $C(T)$  anomaly was previously noted<sup>8</sup>].

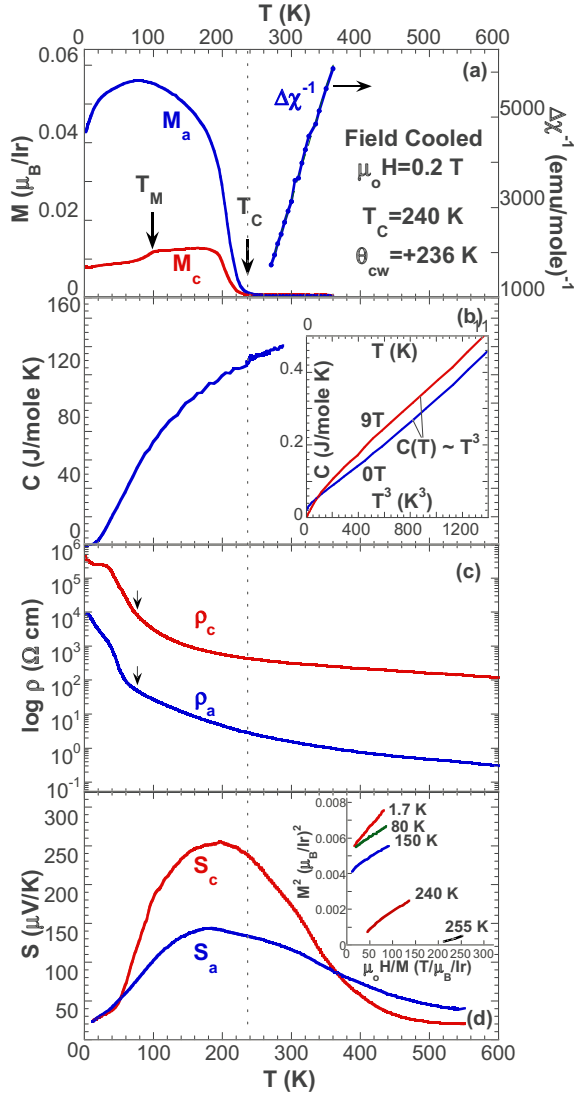


FIG. 1. (Color online) (a) Field-cooled magnetization  $M(T)$  and inverse susceptibility  $\Delta\chi^{-1}(T)$  (right scale) at applied field  $\mu_0 H = 0.2$  T, (b) Specific heat  $C(T)$ , (c) resistivity  $\log \rho(T)$ , and (d) thermoelectric power  $S(T)$  for  $\text{Sr}_2\text{IrO}_4$  as functions of temperature  $T \leq 600$  K. Except for  $C(T)$  ( $H \perp c$ ), all properties are measured for  $H$  along both  $a$  and  $c$  axes. Fig. 1(b) inset:  $C(T)$  vs  $T^3$  for  $T < 11$  K. Fig. 1(d) inset: Arrott plot ( $M^2$  vs  $\mu_0 H/M$ ) shows a FM transition at  $T_C \approx 240$  K. Note: no anomaly is seen in  $\rho(T \approx T_C)$  and  $S(T \approx T_C)$ .

Remarkably, we find no anomaly at  $T_C$  in  $\log \rho(T)$  and  $S(T)$  [Figs. 1(c) and 1(d)], which is perplexing, since the  $M(T \approx T_C)$  anomaly is robust and indicates long-range magnetic order. (Note the transport properties of  $\text{Sr}_2\text{IrO}_4$  are extremely sensitive to oxygen content, but the magnetism is not.<sup>8,14</sup>) The absence of a phase-transition signature in  $\rho(T \approx T_C)$  and  $S(T \approx T_C)$  could reflect a spin-glass state but the real part  $\chi'$  of the ac magnetic susceptibility shown in Fig. 2(a) exhibits no sharp,  $\omega$ -dependent peak near  $T_C$ . It is noted that  $\chi'(T)$  displays a pronounced peak near 135 K and a smaller peak near 85 K, both highly sensitive to dc magnetic field [Fig. 2(a)].

A key feature in Figs. 2(b) and 2(c) is the observed mag-

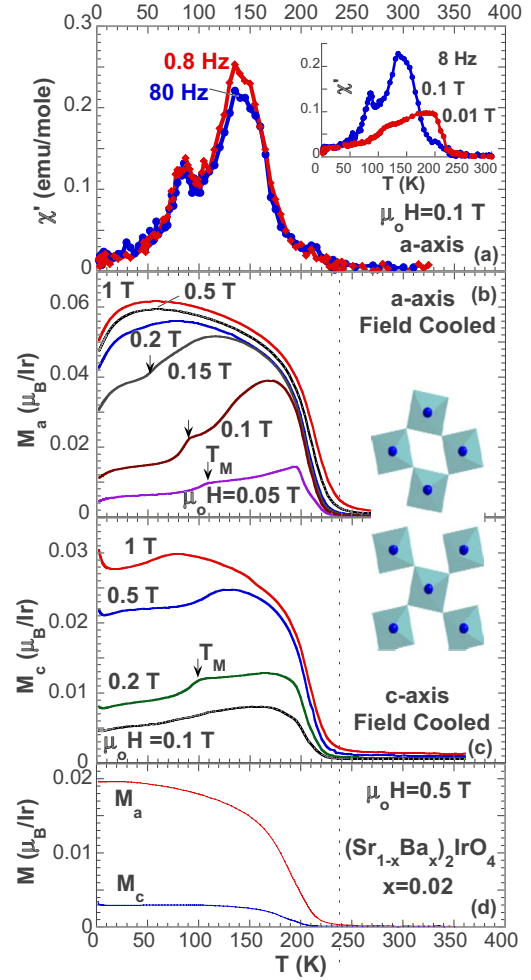


FIG. 2. (Color online) (a) Real part of ac susceptibility  $\chi'(T, \omega)$  along the  $a$  axis at  $\mu_0 H = 0.1$  T and frequencies  $\omega = 0.8$  and 80 Hz. (b) dc magnetizations  $M_a(T)$  and (c)  $M_c(T)$  for various magnetic fields  $H$ . Note the  $H$ -dependent anomaly at  $T_M$  (arrows) (d)  $M(T)$  for  $(\text{Sr}_{1-x}\text{Ba}_x)_2\text{IrO}_4$  with  $x=0.02$  for both the  $a$  and  $c$  axes. Note that  $T_M$  and low- $T$  down turn are no longer visible. Fig. 2(a) inset:  $\chi'(T)$  for  $\omega = 8$  Hz at  $\mu_0 H = 0.01$  and 0.1 T. Figs. 2(b) and 2(c) inset: Rotation scheme for  $\text{IrO}_6$  octahedra.

netic anomaly below  $T_M \approx 100$  K, whose location is very sensitive to  $H$ , and which we argue may be a result of *gradual spin canting*.  $\text{Sr}_2\text{IrO}_4$  crystallizes in the reduced tetragonal space-group  $I4_1/acd$  (Refs. 4 and 5) due to a rotation of the  $\text{IrO}_6$  octahedra about the  $c$  axis by  $\sim 11^\circ$ , which removes the  $I4/mmm$  inversion center existing between the Ir ions along the (100) and (010) directions [inset, Figs. 2(b) and 2(c) (Ref. 4)]. The rotation increases from  $11.36^\circ$  at room temperature to  $11.72^\circ$  at 10 K,<sup>5</sup> corresponding to a reduction in the Ir-O-Ir bond angle from  $157.28^\circ$  to  $156.56^\circ$ , respectively, and accompanies a growth of the  $c$ -axis lattice parameter.<sup>4</sup> Moreover, a strong temperature dependence of bending modes associated with the Ir-O-Ir bond angle was recently observed,<sup>13</sup> which, in turn, influences the magnetic exchange interaction. The data in Fig. 2 suggest that  $T_M$  marks a crossover of the dominant exchange coupling from FM to AFM (discussed earlier), with a reduction in the Ir-O-Ir bond angle. Increased spin canting, or an AFM state, at

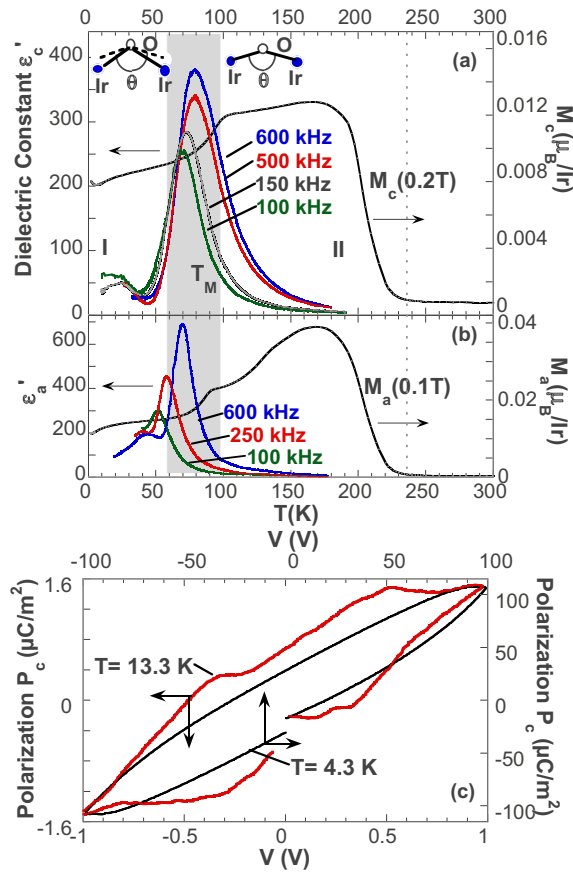


FIG. 3. (Color online) (a) Real part of the  $c$ -axis dielectric constant  $\epsilon'_c(T)$  for representative frequencies  $\omega$  (left scale), and  $c$ -axis magnetization  $M_c(T)$  (right scale); Fig. 3(a) inset: schematic change of O-Ir-O bond angle from region I to region II. (b) Real part of the  $a$ -axis dielectric constant  $\epsilon'_a(T)$  for representative  $\omega$  (left scale), and  $a$  axis  $M_a(T)$  (right scale). (c) Electric polarization  $P$  vs voltage  $V$  for temperature  $T = 13.3$  K (low  $V$ , left scale) and 4.3 K (high  $V$ , right scale).

low  $T$  is also consistent with the downturn in  $M$ , substantial rise in  $\rho(T < T_M)$ , and  $C(T) \propto T^3$  seen at low  $T$  in Fig. 1. It is not surprising that magnetic properties are highly sensitive to impurity doping on either the Sr or Ir site. As shown in Fig. 2(d), 2% Ba substitution for Sr in  $\text{Sr}_2\text{IrO}_4$  completely eliminates all major magnetic features of the pure  $\text{Sr}_2\text{IrO}_4$ , mostly noticeably,  $T_M$  and low- $T$  down turn in  $M$  that are critical to the GME.

Spin canting, the  $T$ -dependent Ir-O-Ir bond angle, and loss of inversion symmetry also influence the dielectric behavior that is strongly dependent on crystal symmetry. Indeed, the magnetic anomaly at  $T_M$  is closely linked to the dielectric response, as shown in Figs. 3(a) and 3(b), where  $M(T)$  is compared to the real parts  $\epsilon'_c(T)$  and  $\epsilon'_a(T)$  of the  $c$  axis and  $a$  axis dielectric constants, respectively. Two major features emerge: (1) both  $\epsilon'_c(T)$  and  $\epsilon'_a(T)$  rise by up to 1 order of magnitude and peak near  $T_M$ , similar to  $\text{La}_2\text{CuO}_4$ .<sup>15</sup> ( $\epsilon_a(T)$  is loss dominated above  $T_M$ , therefore we focus only on  $\epsilon'_c(T)$  in the discussion that follows.) This strong enhancement of  $\epsilon'_c(T)$  is much larger than that exhibited by well-known magnetoelectrics such as  $\text{BaMnF}_4$ ,<sup>16</sup>  $\text{BiMnO}_3$ ,<sup>17</sup>  $\text{HoMnO}_3$  and  $\text{YMnO}_3$ .<sup>18</sup> (2) The peak in  $\epsilon'_c(T \approx T_M)$  separates two regions,

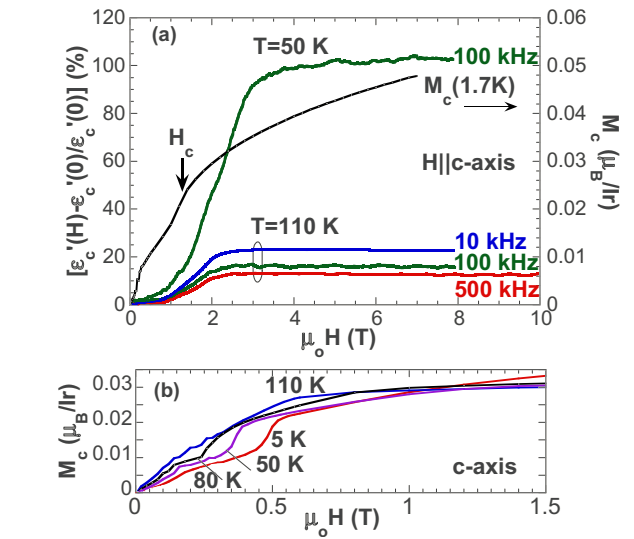


FIG. 4. (Color online) (a) Magnetoelectric effect  $\Delta\epsilon'_c(H)/\epsilon'_c(0)$  along  $c$  axis at temperatures  $T = 50$  and 110 K versus applied field  $H$  for a few representative frequencies  $\omega$  and  $\mu_0 H \leq 10$  T applied along  $c$  axis; Right scale: the  $c$  axis  $M_c(H)$  vs  $H$  at 1.7 K; (b) the  $c$ -axis  $M_c(H)$  at various  $T$ . Note parallel behavior of  $\epsilon_c$  and  $M_c$  near the metamagnetic transition field,  $H_c$ .

I and II, as marked in Fig. 3(a). The weak frequency dependence of  $\epsilon'_c(T, \omega)$  in low- $T$  region I is typical of a ferroelectric, whereas the stronger frequency dependence of  $\epsilon'_c(T, \omega)$  in higher- $T$  region II suggests a relaxor mechanism,<sup>19</sup> which is traditionally attributed to disorder and impurities. Alternatively, the sharp peak accompanied by strong frequency dispersion could signal a frustrated or disordered magnetic state corresponding to the shaded area in Figs. 3(a) and 3(b).

The vast majority of known magnetoelectrics and multiferroics are  $3d$ -based compounds,<sup>15–24</sup> whereas there are no known examples of ferroelectric  $5d$  materials. It is interesting that electric polarization hysteresis is certainly observed in  $\text{Sr}_2\text{IrO}_4$  as shown in Fig. 3(c), suggesting a possible existence of some type of ferroelectric state at low  $T$ . (A detailed description of evidence for the ferroelectric state will be published elsewhere.) Furthermore, a magnetodielectric shift  $\Delta\epsilon'_c(H)/\epsilon'_c(0)$  is also anticipated and observed in  $M_c(H)$  near the metamagnetic transition field  $H_c$  (Fig. 4). (The negligible magnetoresistance in  $\text{Sr}_2\text{IrO}_4$  at  $H$  up to 12 T (Ref. 7) suggests that  $\Delta\epsilon'_c(H)/\epsilon'_c(0)$  is an intrinsic effect.) However, we do not observe  $\Delta\epsilon'_c(H) \propto M^2$  as conventionally expected,<sup>7</sup> and  $M (< 0.1 \mu_B/\text{Ir})$  is exceptionally weak compared to known multiferroics [e.g.,  $M \approx 6 \mu_B/\text{f.u.}$  for  $\text{TbMnO}_3$  (Ref. 23)].

Although the GME in  $\text{Sr}_2\text{IrO}_4$  is unconventional, it can be understood as a unique manifestation of a recently formulated microscopic mechanism for magnetoelectrics with strong spin-orbit coupling; this approach yields polarization  $P$  proportional to an effective spin-orbit gap  $\Delta_s$  rather than the magnitude and spatial dependence of the magnetization.<sup>12</sup>

In light of all results presented above, it is suggested that  $T_M$  defines a drastic change in the coupling between the magnetic and dielectric response, according to the following sce-

nario: In Region II, the strong competition between FM and AFM exchange couplings promotes frustrated or incommensurate magnetic order. A  $T$ -dependent magnetoelastic coupling may give rise to a soft lattice mode, as indicated by optical data<sup>13</sup> and the weak frequency dependence of  $\chi'$  near 135 K [Fig. 2(a)]. The Ir-O-Ir bond angle [Fig. 3(a)] decreases with decreasing  $T$ , strengthening the AFM exchange coupling until, near  $T_M$ , the AFM coupling becomes dominant, and spins are “locked in” with a stiffened lattice in region I. This scenario explains (a)  $C(T) \propto T^3$  below 11 K [Fig. 1(b)], (b) the low- $T$  downturn in  $M$  [Figs. 1(a) and 2(b)], (c) the rise of  $\rho(T)$  below  $T_M$  [Fig. 1(c)], (d) the reduction in the frequency dependence of  $\epsilon'_c(T, \omega)$  in region I [Fig. 3(a)], and (e) the reduction in the magnetodielectric effect  $\Delta\epsilon'_c(H)/\epsilon'_c(0)$  from 100% at 50 K, to only 21% at 110 K [Fig. 4(a)].

In summary, a dominant spin-orbit coupling in  $\text{Sr}_2\text{IrO}_4$  shifts the balance of competing magnetic, dielectric and lattice energies, generating a type of GME that is not dependent on the magnetization, but nevertheless is intimately linked with the complex magnetic order emerging from an exotic Mott insulating state. We expect further examples of exciting type of GME and possible multiferroics to be found in other  $5d$  Mott insulators.

This work was supported by NSF through Grant Nos. DMR-0552267, DMR-0856234, and EPS-0814194. L.E.D. was supported by the U.S. DOE through Grant No. DE-FG02-97ER45653. P.S. was supported by the U.S. DOE through Grant No. DE-FG02-98ER45707.

\*Corresponding author; cao@pa.uky.edu

- <sup>1</sup>G. Cao, J. E. Crow, R. P. Guertin, P. F. Henning, C. C. Homes, M. Strongin, D. N. Basov, and E. Lochner, *Solid State Commun.* **113**, 657 (2000).
- <sup>2</sup>G. Cao, X. N. Lin, S. Chikara, V. Durairaj, and E. Elhami, *Phys. Rev. B* **69**, 174418 (2004).
- <sup>3</sup>K. Maiti, R. S. Singh, V. R. R. Medicherla, S. Rayaprol, and E. V. Sampathkumaran, *Phys. Rev. Lett.* **95**, 016404 (2005).
- <sup>4</sup>M. K. Crawford, M. A. Subramanian, R. L. Harlow, J. A. Fernandez-Baca, Z. R. Wang, and D. C. Johnston, *Phys. Rev. B* **49**, 9198 (1994).
- <sup>5</sup>Q. Huang, J. L. Soubeyroux, O. Chmaisnen, I. Natali Sora, A. Santoro, R. J. Cava, J. J. Krajewski, and W. F. Peck, Jr., *J. Solid State Chem.* **112**, 355 (1994).
- <sup>6</sup>R. J. Cava, B. Batlogg, K. Kiyono, H. Takagi, J. J. Krajewski, W. F. Peck, L. W. Rupp, and C. H. Chen, *Phys. Rev. B* **49**, 11890 (1994).
- <sup>7</sup>G. Cao, J. Bolivar, S. McCall, J. E. Crow, and R. P. Guertin, *Phys. Rev. B* **57**, R11039 (1998).
- <sup>8</sup>N. S. Kini, A. M. Strydom, H. S. Jeevan, C. Geibel, and Ramakrishnan, *J. Phys: Condens. Matter* **18**, 8205 (2006).
- <sup>9</sup>B. J. Kim, H. Jin, S. J. Moon, J.-Y. Kim, B.-G. Park, C. S. Leem, J. Yu, T. W. Noh, C. Kim, S.-J. Oh, J. H. Park, V. Durairaj, G. Cao, and E. Rotenberg, *Phys. Rev. Lett.* **101**, 076402 (2008).
- <sup>10</sup>G. Cao, Y. Xin, C. S. Alexander, J. E. Crow, P. Schlottmann, M. K. Crawford, R. L. Harlow, and W. Marshall, *Phys. Rev. B* **66**, 214412 (2002).
- <sup>11</sup>S. J. Moon, H. Jin, K. W. Kim, W. S. Choi, Y. S. Lee, J. Yu, G. Cao, A. Sumi, H. Funakubo, C. Bernhard, and T. W. Noh, *Phys. Rev. Lett.* **101**, 226402 (2008).
- <sup>12</sup>J. Hu, *Phys. Rev. Lett.* **100**, 077202 (2008).
- <sup>13</sup>S. J. Moon, W. S. Choi, J. S. Lee, S. S. A. Seo, T. W. Noh, H. Jin, J. Yu, G. Cao, and Y. S. Lee (unpublished).
- <sup>14</sup>Our recent studies indicate that a slight change in oxygen stoichiometry can drastically change the resistivity by a few orders of magnitude, but no parallel changes are seen in magnetic properties.
- <sup>15</sup>G. Cao, J. W. O'Reilly, J. E. Crow, and L. R. Testardi, *Phys. Rev. B* **47**, 11510 (1993).
- <sup>16</sup>J. F. Scott, *Phys. Rev. B* **16**, 2329 (1977).
- <sup>17</sup>T. Kimura, S. Kawamoto, I. Yamada, M. Azuma, M. Takano and Y. Tokura, *Phys. Rev. B* **67**, 180401(R) (2003).
- <sup>18</sup>B. Lorenz, Y. Q. Wang, Y. Y. Sun, and C. W. Chu, *Phys. Rev. B* **70**, 212412 (2004).
- <sup>19</sup>G. Samara, in *Solid State Physics*, edited by H. Ehrenreich and F. Spaepen (Academic Press, New York, 2001), Vol. 56, p. 270.
- <sup>20</sup>N. A. Hill, *J. Phys. Chem. B* **104**, 6694 (2000).
- <sup>21</sup>N. Hur, S. Park, P. A. Sharma, J. S. Ahn, S. Guha, and S.-W. Cheong, *Nature (London)* **429**, 392 (2004).
- <sup>22</sup>W. Eerenstein, N. D. Mathur, and J. F. Scott, *Nature (London)* **442**, 759 (2006).
- <sup>23</sup>T. Kimura, *Annu. Rev. Mater. Res.* **37**, 387 (2007).
- <sup>24</sup>R. Ranjith, A. K. Kunu, M. Filippi, B. Kundys, W. Prellier, B. Ravaeu, J. Lavediere, M. P. Singh, and S. Jandl, *Appl. Phys. Lett.* **92**, 062909 (2008).